

# Discovery of an Overlapping Cluster in Abell 1674 Field with Suzaku

Shota INOUE,<sup>1</sup> Kiyoshi HAYASHIDA,<sup>1</sup> Hiroki AKAMATSU,<sup>2</sup> Shutaro UEDA,<sup>1</sup> Ryo NAGINO,<sup>1</sup>  
Hiroshi TSUNEMI,<sup>1</sup> Noriaki TAWA,<sup>1</sup> and Katsuji KOYAMA<sup>1,3</sup>

<sup>1</sup>*Department of Earth and Space Science, Graduate School of Science, Osaka University,  
1-1 Machikaneyama-cho, Toyonaka, Osaka 560-0043*

<sup>2</sup>*SRON Netherlands Institute for Space Research, Sorbonnelaan 2, 3584 CA Utrecht, The Netherlands*

<sup>3</sup>*Department of Physics, Graduate School of Science, Kyoto University,  
Kitashirakawa Oiwake-cho, Sakyo-ku, Kyoto 606-8502  
shota@ess.sci.osaka-u.ac.jp*

(Received 2014 February 13; accepted 2014 May 1)

## Abstract

We present the results of a Suzaku observation of Abell 1674, an optically very rich (richness class 3) cluster cataloged as  $z = 0.1066$ . We discover the He-like Fe K-shell line from the central region for the first time, and find that the X-ray spectrum yields a high redshift of  $0.215_{-0.006}^{+0.007}$ . On the other hand, the spectrum of the southwestern region is fitted with a redshift of  $0.11 \pm 0.02$  by the He-like Fe L-shell lines, consistent with the optically determined value. The gas temperature, metal abundance, and core radius of the X-ray emission in the central region are  $3.8 \pm 0.2$  keV,  $0.20 \pm 0.05 Z_{\odot}$  and  $450 \pm 40$  kpc, respectively, while those in the southwestern region are  $2.0 \pm 0.2$  keV,  $0.41_{-0.13}^{+0.17} Z_{\odot}$  and  $220_{-70}^{+90}$  kpc, respectively. These parameters are typical for clusters. We thus conclude that Abell 1674 consists of two independent clusters, A1674-C at  $z \sim 0.22$  and A1674-SW at  $z \sim 0.11$ , overlapping along the line of sight. The X-ray luminosities of A1674-C within  $r = 2$  Mpc is  $15.9 \pm 0.6 \times 10^{43} \text{ erg s}^{-1}$  in the 0.1–2.4 keV energy band, while that for A1674-SW is  $1.25 \pm 0.07 \times 10^{43} \text{ erg s}^{-1}$ . Both are consistent with those expected from the  $L - T$  relation of clusters within a factor of 2. This is another support for our conclusion.

**Key words:** galaxies: clusters: individual: Abell 1674 — galaxies: clusters: intracluster medium — X-rays: galaxies: clusters — X-rays: individuals: Abell 1674

## 1. Introduction

Abell 1674 (hereafter A1674) was listed in the cluster catalogs by Abell (1958) and Abell et al. (1989) as a richness class 3 cluster. The redshift of A1674 was determined to be 0.1055 by Schneider, Gunn and Hoessel (1983) from the redshift of 1 member galaxy, and is cited in the ACO catalog (Abell et al. 1989). Struble and Rood (1999) reported the redshift to be  $z = 0.1066$  based on the measurement of 2 member galaxies by Huchra et al. (1990).

The X-ray luminosity measured with ROSAT is  $L = 2.55 \times 10^{43} \text{ ergs}^{-1}$  within  $r = 1.1 \text{ Mpc}$  in the  $0.5 - 2.5 \text{ keV}$  band (Briel & Henry 1993). In this paper, we use the Hubble constant  $H_0 = 70 \text{ kms}^{-1} \text{ Mpc}^{-1}$ ,  $\Omega_m = 0.2$  and  $\Omega_\Lambda = 0.8$ . The metal abundance is reported with the ASCA and XMM-Newton observations (Hashimoto et al. 2000 and Katayama, Hayashida and Nishino 2005), and is less than  $0.2 Z_\odot$ . These two parameters are significantly lower than the typical values of clusters of galaxies of this richness class (e.g., Briel & Henry 1993, Leccardi & Molendi 2008). They thus suggested that metals have not yet been supplied to the hot intracluster medium (ICM), and speculated that A1674 is at an early evolutionary stage (Hashimoto et al. 2000; Katayama, Hayashida and Nishino 2005). We report the result of the Suzaku satellite (Mitsuda et al. 2007) observation using the X-ray Imaging Spectrometer (XIS, Koyama et al. 2007) to investigate these unusual X-ray properties of the ICM in A1674.

## 2. Observation and Data Reduction

The observation was performed for an effective exposure of 68 ks on 2006 December 16. Suzaku has four XIS Cameras; three of the XIS (XIS 0, 2, 3) employ front-illuminated (FI) CCDs, and a back-illuminated CCD is installed in the other (XIS 1). Since XIS 2 has been out of function from 2006 November 9, we use the remaining three XIS (XIS 0, 1, 3). The observation was performed with either the normal  $3 \times 3$  or  $5 \times 5$  mode. These data are combined. Figure 1 shows the X-ray image of A1674. In addition to the bright central emission, faint point-like sources in the east, and diffuse emissions in the northeast and southwest are observed.

## 3. Analysis and Results

We extracted the X-ray spectra using XSELECT ver.2.4. The non-X-ray background (NXB) was produced with the FTOOL *xisnxbgen* (Tawa et al. 2008), using the night-earth data taken before and after 150 days of our observation. The NXB was subtracted from the source spectra, while the X-ray background (XB) was included in the spectral fitting. The response matrix files were generated by the FTOOL *xisrmfgen*. The auxiliary response files (ARFs) were generated by *xissimarfgen* with the observed image of A1674 in the  $0.5 - 2 \text{ keV}$  band (Ishisaki et al. 2007). We analyzed the spectra in the  $0.4 - 8.0 \text{ keV}$  and the  $0.25 - 7.0 \text{ keV}$  bands for the FI CCDs and the BI CCD, respectively.

### 3.1. Spectral Analysis of the Central Region

We extracted the X-ray spectrum of the central region of the radius of  $4'$  with the center position at  $(\alpha, \delta) = (196^\circ 0035, 67^\circ 5164)$ . The spectra after the NXB subtraction are shown in Fig. 2. The spectral model includes the X-ray background (XB) in addition to the ICM. The XB consists of the cosmic X-ray background (CXB), the Milky Way halo (MWH) and the local hot bubble (LHB). The spectrum of the CXB is assumed to be a *powerlaw* model with the parameters presented by Kushino et al. (2002). The emissions from the MWH and LHB are modeled with a XSPEC model *apec* (Smith et al. 2001) with metal abundances of  $1 Z_\odot$ . We report the metal abundances relative to the solar values in Anders and Grevesse (1989).

We apply the *apec* model for the ICM spectra. The absorption is given by the *wabs* model (Morrison & McCammon 1983), where the hydrogen column density is fixed to  $N_H = 1.7 \times 10^{20} \text{ cm}^{-2}$  (Kalberla et al. 2005). All together, our spectral model is [*apec*(ICM) + *powerlaw*(CXB) + *apec*(MWH)] \* *wabs* + *apec*(LHB).

In the fitting, we first fixed the redshift to be  $z = 0.1066$  as suggested by the optical data (Struble & Rood 1999). Figure 2 (a) shows the best-fit models. The best-fit temperature and metal abundances of the ICM are  $3.6_{-0.3}^{+0.2} \text{ keV}$  and  $0.04 \pm 0.04 Z_\odot$ , respectively. These are consistent with the previous observations (Hashimoto-dani et al. 2000; Katayama, Hayashida and Nishino 2005). However in Fig. 2 (a), we see a clear line-like residual at around 5.5 keV, possibly redshifted iron K-shell line. We then allowed the redshift to be a free parameter. The best-fit model is shown in Fig. 2 (b), while the best-fit parameters are summarized in Table 1. This fit well reproduces the line-like structure at around 5.5 keV, as the redshifted ( $z = 0.215_{-0.006}^{+0.007}$ ) iron K-shell line. Using the F-test, decrease in  $\chi^2$  is highly significant with a null hypothesis probability of  $4 \times 10^{-13}$ . This is the first detection of the iron K-shell line from A1674. The metal abundance of the Center region is  $0.20 \pm 0.05 Z_\odot$ , which is not unusual for clusters. Obviously, the statistics of the previous X-ray observations (Hashimoto-dani et al. 2000; Katayama, Hayashida and Nishino 2005) were too poor to determine the reliable redshift and metal abundance.

### 3.2. Spectral Analysis of the Southwestern Region

Since the X-ray redshift of the A1674 Center region ( $z = 0.215_{-0.006}^{+0.007}$ ) is different from that determined optically, we examine the spatial distribution of optical galaxies near and around A1674. Figure 3 (a) shows the galaxy distribution on the Suzaku X-ray image of A1674 taken from the Sloan Digital Sky Survey (SDSS, York et al. 2000) database, while Fig. 3 (b) is the redshift-sorted galaxy distribution made from the SDSS spectroscopic survey list. Although the SDSS spectroscopic survey is not deep enough to include most of the galaxies with  $z \sim 0.2$  in this region (Strauss et al. 2002), we see three galaxies with  $0.21 < z < 0.23$  in the Center region. On the other hand, eight galaxies with  $0.10 < z < 0.12$  are found in the southwestern region. We find two separated structures in the X-ray emission in the southwestern region. We thus define

two extraction regions, SW1 and SW2, marked by the solid blue line in Fig. 3. The center coordinate of SW1 and that in SW2 are  $(\alpha, \delta) = (195^\circ 6696, 67^\circ 4784)$  and  $(195^\circ 8993, 67^\circ 4470)$ , respectively. The X-ray emissions in SW1 and SW2 are more extended than the point-spread function (PSF) of the X-ray telescope on board Suzaku (Serlemitsos et al. 2007).

We employ similar data reduction and analysis for the spectra of SW1 and SW2 regions to those of the Center region (Section 3.1). Since the X-ray emission in each SW region is far fainter than that in the Center region, contamination (pile-over) from the Center region should be taken into account. We estimate it by using the best-fit spectral parameters in Table 1 and the ARFs of which source region is set at the Center region. We also have to take the mutual contamination between SW1 and SW2 into account. The spectra of SW1 and SW2 are thus fitted simultaneously. Figure 4 shows the NXB-subtracted spectra of SW1 and SW2 with their best-fit models. The best-fit parameters are summarized in Table 2. In the SW1 region, the He-like Fe L-shell emissions around 1 keV determine the redshift to be  $z = 0.11 \pm 0.02$ , which is consistent with  $z = 0.1066$  obtained from the optical observation (Struble & Rood 1999). The temperature and metal abundance are  $2.0 \pm 0.2$  keV and  $0.41^{+0.17}_{-0.13} Z_\odot$ . The temperature is significantly lower than that in the Center region. The metal abundance is marginally different from that in the Center region but is typical for clusters.

On the other hand, the X-ray spectrum of the SW2 region shows no apparent line-like structures. This is partly due to its lower surface brightness than the SW1 region and also to the strong contamination from the Center region; the contamination from the Center region is comparable to the intrinsic emission from the SW2 region. We thus conclude that the X-ray spectral property of the SW2 region is hard to be constrained with this observation.

### 3.3. Radial Profiles

Spatial structures of the extended X-ray emission in the Center region and the SW1 region are examined by fitting their radial profiles with a  $\beta$ -model (Cavaliere & Fusco-Femiano 1978). This procedure is also needed to evaluate their X-ray luminosities. Radial profiles were derived from the X-ray image shown in Figure 1. The radial profiles derived in this way are those convolved with the Suzaku PSF. We thus estimate the Suzaku PSF with the FTOOL *xissimarfgn* and convolve a  $\beta$ -model with the PSF to fit the radial profile, as was done by Mori et al. 2013.

Figure 5 (a) shows the radial profile in the Center region with the best-fit model, whose parameters are in the column 1 of Table 3. We confirm the emission of the Center region extends at least to 1.3 Mpc from the center. The core radius  $r_c$  and  $\beta$  is  $450 \pm 40$  kpc and  $0.52 \pm 0.04$ , respectively. According to the analysis of a large sample of clusters (e.g. Mohr et al. 1999, Ota & Mitsuda 2004, Akahori & Masai 2006, Ota et al. 2006),  $r_c$  and  $\beta$  are in 20 – 800 kpc and in 0.2 – 1.2, respectively. It indicates that  $r_c$  and  $\beta$  of the Center region are within these ranges. Figure 5 (b) shows the radial profile of A1674-SW with the best-fit model, whose parameters

are in the column 2 of Table 3. We find the  $\beta$ -model component dominates the background emission up to  $\sim 0.4$  Mpc in the SW1 region. The core radius  $r_c$  and  $\beta$  of the SW1 region is  $220^{+90}_{-70}$  kpc and  $0.9^{+0.4}_{-0.2}$ , respectively. These values are also consistent with other clusters. We find some deviation of the radial profile in the SW1 region from the best fit  $\beta$ -model. The profile is better reproduced with a double  $\beta$ -model. Although we employ the single  $\beta$ -model fit in the following discussion, we note that the integrated X-ray luminosity based on it is lower than that with the double  $\beta$ -model fit by about 10%.

#### 4. Discussion

As described in Sec. 3, we find two different redshifts,  $0.215^{+0.007}_{-0.006}$  and  $0.11 \pm 0.02$ , from the two separate regions (the Center and SW1 regions) in the field of A1674. This redshift difference corresponds to  $\sim 30,000$  km s $^{-1}$ , which is too large to be attributed to a bulk motion in one cluster. We therefore can safely conclude that A1674 consists of at least two independent clusters overlapping along the line of sight. In the following discussion, we name these clusters A1674-C and A1674-SW. We conventionally call A1674-SW a cluster in this paper, although we may had better call it a group of galaxies, considering its lower temperature of  $2.0 \pm 0.2$  keV. Note also that we were not able to constrain the spectral properties of the faint X-ray emission in the SW2 region.

Our hypothesis that A1674 is separated into two independent clusters of A1674-C and A1674-SW is supported by the spatial distribution of galaxies between  $0.10 < z < 0.12$  and  $0.21 < z < 0.23$  as shown in Fig. 3 (b). Although the SDSS spectroscopic survey is not deep enough to detect many galaxies with  $z \sim 0.2$  (Strauss et al. 2002), most of the galaxies measured in the SDSS spectroscopic survey are spatially separated into two groups of  $0.21 < z < 0.23$  (A1674-C) and  $0.10 < z < 0.12$  (A1674-SW). The separation is, however, not clear, and there are some overlaps. For example, we find one galaxy with  $0.21 < z < 0.23$  in the SW1 region. The galaxy is at a distance of 1.24 Mpc from the center of A1674-C. Assuming the distribution of galaxies follows the X-ray radial profile we measured, the ratio of the number of galaxies inside and outside 1.1 Mpc should be about 3:2, which is statistically consistent with what we observe. We hence consider that this galaxy is most likely a member of A1674-C. On the other hand, we find one galaxy with  $0.10 < z < 0.12$  in the Center region. The galaxy is at a distance of 1.26 Mpc from the center of A1674-SW. Since we only confirmed the X-ray emission of A1674-SW up to  $\sim 0.4$  Mpc, the galaxy may not be a member of A1674-SW but a field galaxy. Deeper spectroscopic observations of galaxies in the field of A1674 are needed for further discussions of optical properties of these clusters.

X-ray properties (temperature, core radius, and  $\beta$ ) of A1674-C and A1674-SW are within the range of those observed for other clusters, as described in Sec. 3. The X-ray luminosity of each cluster is evaluated with their radial profiles described in Sec. 3.3. If we extrapolate the radial profile up to  $r = 2$  Mpc, we obtain the X-ray luminosity (0.1 – 2.4 keV within 2 Mpc) of

A1674-C to be  $L = 15.9 \pm 0.6 \times 10^{43} \text{ ergs}^{-1}$ , while that of A1674-SW is  $1.25 \pm 0.07 \times 10^{43} \text{ ergs}^{-1}$ . If we limit the outer radius to be 1.3 Mpc and 0.4 Mpc for A1674-C and A1674-SW, respectively, the X-ray luminosities of these two clusters are  $13.6 \pm 0.5 \times 10^{43} \text{ ergs}^{-1}$  and  $1.08 \pm 0.06 \times 10^{43} \text{ ergs}^{-1}$ , respectively. On the other hand, expected luminosities within 2 Mpc from the observed temperatures (3.8 keV for A1674-C and 2.0 keV for A1674-SW) using the  $L-T$  relation (equation (4) in Ikebe et al. 2002), are  $7.9 \times 10^{43} \text{ ergs}^{-1}$  and  $1.6 \times 10^{43} \text{ ergs}^{-1}$ . These are consistent with the observed luminosities within a factor of 2, which is comparable to or smaller than the scatters of the data points found in Ikebe et al. (2002). This is another support for our hypothesis.

New clusters of galaxies were serendipitously discovered or identified with Suzaku observations, as reported by Yamauchi et al. (2010), Yamauchi et al. (2011) and Mori et al. (2013). In either case, an iron emission line in the X-ray spectra and an extended X-ray emission are the key to identify the source as a cluster. The discovery of the new cluster of galaxies A1674-C is similar to those previous cases but from the previously cataloged cluster A1674.

## 5. Summary

We performed a spectral and spatial analysis for the cluster of galaxies A1674 in separate regions observed with Suzaku. We discovered the He-like Fe K-shell line from the Center region of this cluster for the first time, and find that the X-ray spectrum yields a higher redshift of  $0.215_{-0.006}^{+0.007}$  than 0.1066 that determined in the optical observations. On the other hand, the X-ray spectrum of the SW1 region is fitted with a redshift of  $0.11 \pm 0.02$ , primarily determined with the He-like Fe L-shell lines. The galaxies in the SDSS spectroscopic survey data also shows two separate component in the redshifts and spatial distributions. We hence conclude that A1674 consists of two independent clusters of galaxies, A1674-C and A1674-SW, overlapping along the line of sight. The gas temperature, metal abundance, core radius,  $\beta$  of A1674-C are  $3.8 \pm 0.2 \text{ keV}$ ,  $0.20 \pm 0.05 Z_{\odot}$ ,  $450 \pm 40 \text{ kpc}$ , and  $0.52 \pm 0.04$ , respectively. Those of A1674-SW are  $2.0 \pm 0.2 \text{ keV}$ ,  $0.41_{-0.13}^{+0.17} Z_{\odot}$ ,  $220_{-70}^{+90} \text{ kpc}$ , and  $0.9_{-0.2}^{+0.4}$ , respectively. These parameters are within the range of those observed in other clusters. The X-ray luminosities evaluated for A1674-C and A1674-SW are consistent with those expected from their temperatures by using the  $L-T$  relation described in Ikebe et al. (2002) within a factor of 2. These are additional supports for our conclusion that A1674 consists of two independent clusters of galaxies.

Previous optical determination of the redshift of A1674 based on measurements of two member galaxies by Huchra et al. (1990) turned out to be not enough for this kind of overlapping system. X-ray observations with high signal to noise ratio are efficient to find different redshift components in clusters.

## Acknowledgments

We thank all members of the Suzaku operation and calibration teams. This work is supported by Japan Society for the Promotion of Science (JSPS) KAKENHI Grant Number 23340071 (Kiyoshi Hayashida), 12J01190 (Shutaro Ueda), 23000004 (Hiroshi Tsunemi), 24540229 (Katsuji Koyama). SRON is also supported financially by NWO, the Netherlands Organization for Scientific Research. H.A. is supported by a Grant-in-Aid for Japan Society for the Promotion of Science (JSPS) Fellows (26-606).

## References

- Abell, G. O. 1958, *ApJS*, 3, 211
- Abell, G. O., Corwin, H. G., Jr., & Olowin, R. P. 1989, *ApJS*, 70, 1
- Akahori, T., & Masai, K. 2006, *PASJ*, 58, 521
- Anders, E., & Grevesse, N. 1989, *Geochim. Cosmochim. Acta*, 53, 197
- Briel, U. G., & Henry, J. P. 1993, *A&A*, 278, 379
- Cavaliere, A., & Fusco-Femiano, R. 1978, *A&A*, 70, 677
- Hashimoto-dani, K., Hayashida, K., Takai, T., Kawasaki, W., & Takeuchi, T. T. 2000, *Advances in Space Research*, 25, 611
- Huchra, J. P., Henry, J. P., Postman, M., & Geller, M. J. 1990, *ApJ*, 365, 66
- Ikebe, Y., Reiprich, T. H., Böhringer, H., Tanaka, Y., & Kitayama, T. 2002, *A&A*, 383, 773
- Ishisaki, Y., et al. 2007, *PASJ*, 59, 113
- Kalberla, P. M. W., Burton, W. B., Hartmann, D., Arnal, E. M., Bajaja, E., Morras, R., & Pöppel, W. G. L. 2005, *A&A*, 440, 775
- Katayama, H., Hayashida, K., & Nishino, Y. 2005, *Advances in Space Research*, 36, 689
- Koyama, K., et al. 2007, *PASJ*, 59, 23
- Kushino, A., Ishisaki, Y., Morita, U., Yamasaki, N., Ishida, M., Ohashi, T., & Ueda, Y. 2002, *PASJ*, 54, 327
- Leccardi, A., & Molendi, S. 2008, *A&A*, 487, 461
- Mitsuda, K., et al. 2007, *PASJ*, 59, 1
- Mohr, J. J., Mathiesen, B., & Evrard, A. E. 1999, *ApJ*, 517, 627
- Mori, H., Maeda, Y., Furuzawa, A., Haba, Y., & Ueda, Y. 2013, *PASJ*, 65, 102
- Morrison, R., & McCammon, D. 1983, *ApJ*, 270, 119
- Ota, N., & Mitsuda, K. 2004, *A&A*, 428, 757
- Ota, N., Kitayama, T., Masai, K., & Mitsuda, K. 2006, *ApJ*, 640, 673
- Schneider, D. P., Gunn, J. E., & Hoessel, J. G. 1983, *ApJ*, 264, 337
- Serlemitsos, P. J., et al. 2007, *PASJ*, 59, 9
- Smith, R. K., Brickhouse, N. S., Liedahl, D. A., & Raymond, J. C. 2001, *ApJL*, 556, L91
- Strauss, M. A., et al. 2002, *AJ*, 124, 1810
- Struble, M. F., & Rood, H. J. 1999, *ApJS*, 125, 35
- Tawa, N., et al. 2008, *PASJ*, 60, 11
- Yamauchi, S., Ueno, M., Bamba, A., & Koyama, K. 2010, *PASJ*, 62, 219
- Yamauchi, S., Bamba, A., & Koyama, K. 2011, *PASJ*, 63, 957
- York, D. G., et al. 2000, *AJ*, 120, 1579

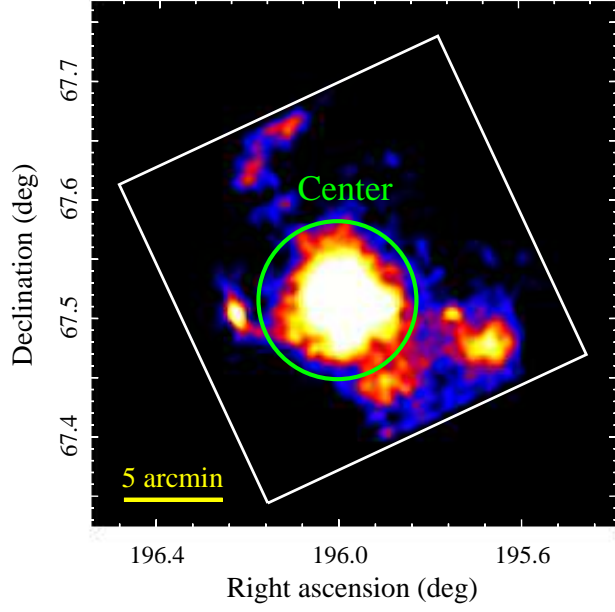


**Fig. 1.** X-ray image of A1674, the sum of the XIS 0, XIS 1 and XIS 3 data. The energy ranges of the data of the FI CCDs are 0.4 – 10 keV, while that of the BI CCD is 0.25 – 8 keV. The green circle indicates the Center region defined in Sec. 3.1. The yellow solid line and the white box represent a 5 arcmin scale and the Suzaku field of view, respectively.

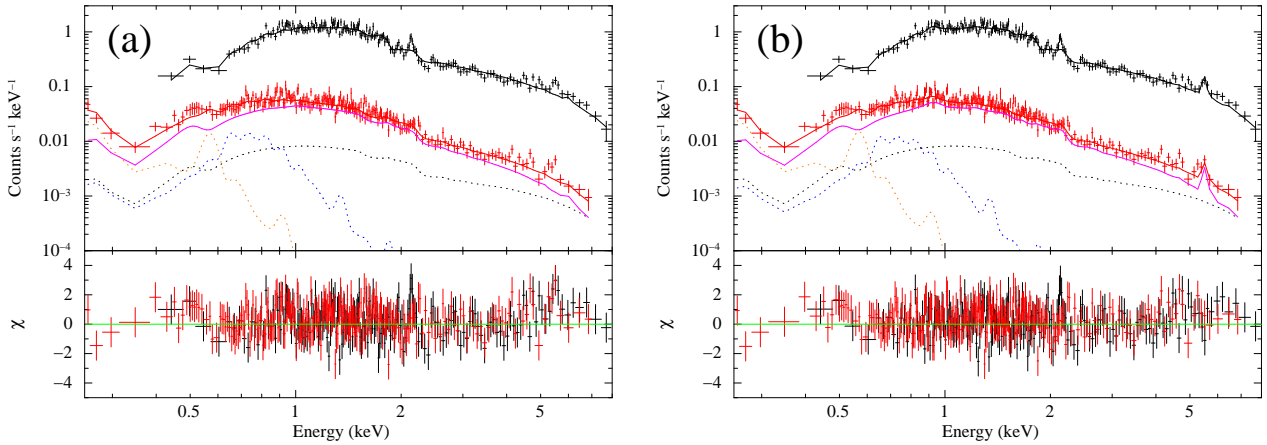


**Fig. 2.** Spectra of the Center region after the subtraction of the NXB. The FI (black) and BI (red) spectra are fitted simultaneously with the model of ICM (magenta solid line) + CXB (black dashed line) + MWH (blue dashed line) + LHB (orange dashed line). The FI spectrum is multiplied by 30 for display purpose. In (a), we perform a model fit with fixing  $z = 0.1066$ , while (b) is redshift of the ICM of a free parameter.

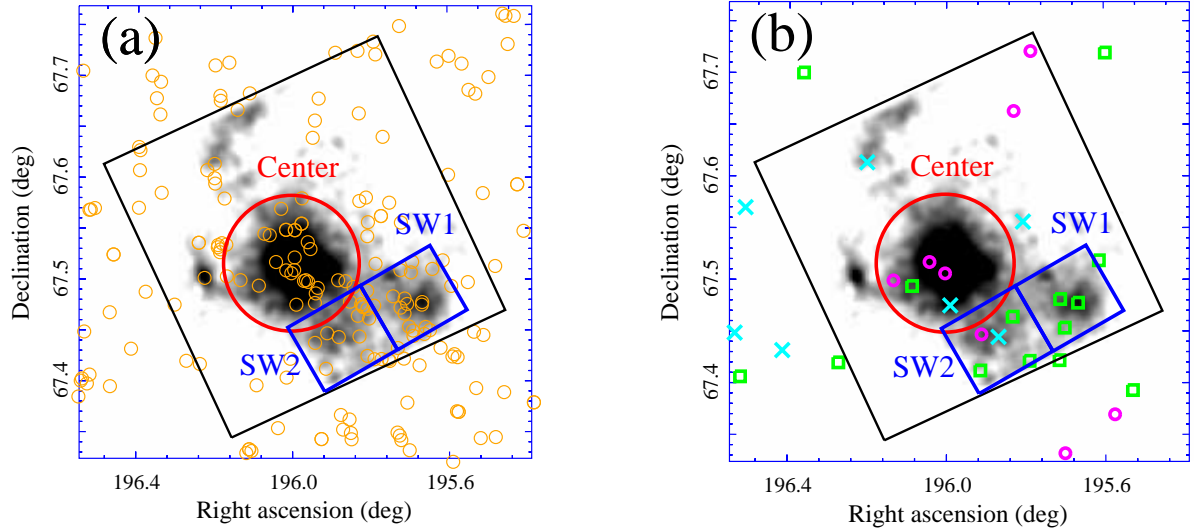


**Fig. 3.** Galaxies observed in the SDSS plotted overlaid on the X-ray image of A1674. The red circle, two blue boxes and black box represent the Center, SW1, SW2 region and the Suzaku field of view, respectively. (a): The orange circles indicate galaxies listed in the SDSS photometry catalog, and are selected under the condition that all the magnitudes of the  $g$ ,  $r$ ,  $i$ , and  $z$  bands are brighter than 20. (b): Same as (a), but is redshift-sorted galaxy distribution. The green squares and magenta circles are galaxies with  $0.10 < z < 0.12$  and those with  $0.21 < z < 0.23$ , respectively. The galaxies with the other redshifts are indicated by cyan crosses.

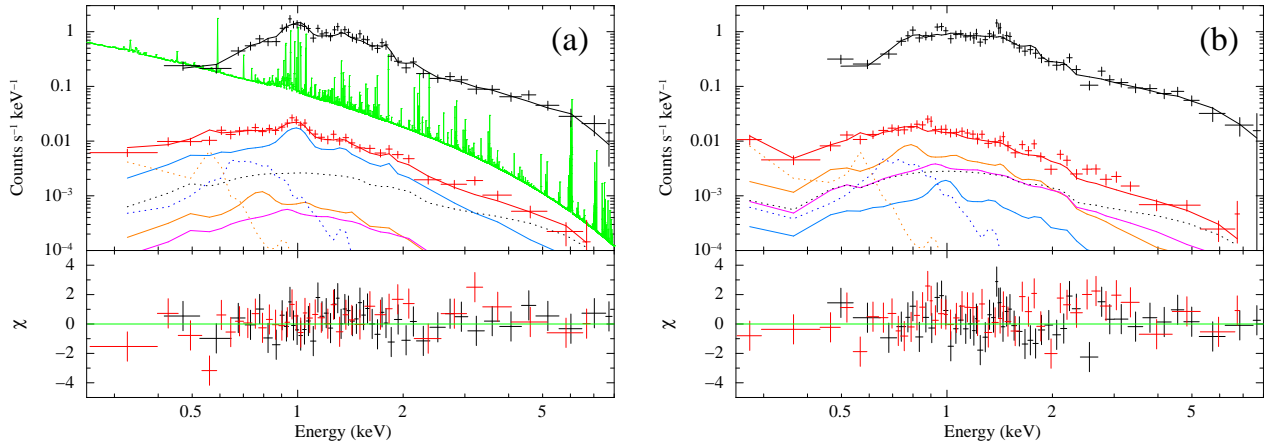


**Fig. 4.** Spectra of the SW1 (left) and SW2 (right) region after the subtraction of the NXB. The FI (black) and BI (red) spectra are simultaneously fitted with a model of the ICM + CXB (black dashed line) + MWH (blue dashed line) + LHB (orange dashed line) + [contamination from another region]. The blue, orange and magenta solid lines indicate a component of emission or contamination from the SW1 region, that from SW2 and that from Center, respectively. The green line of the left panel represents the unfolded model of the component of emission from the SW1 region in the arbitrary unit. The FI spectrum is multiplied by 100 for display purpose.

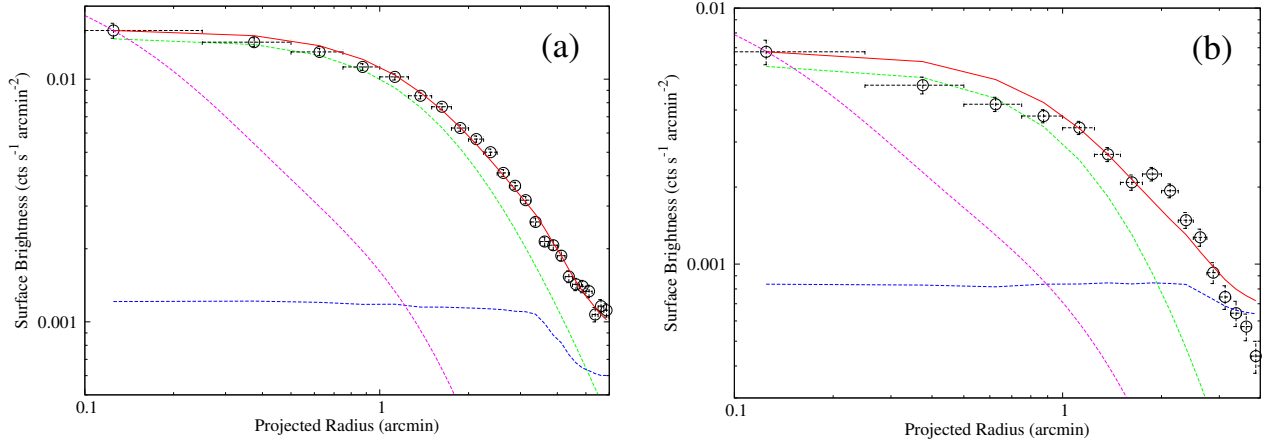


**Fig. 5.** X-ray surface brightness in the Center (left) and SW1 (right) regions (open circles). The X-ray image of Fig. 1 (energy ranges are 0.4 – 10 keV for the FI-CCDs and 0.25 – 8 keV for the BI-CCD) is employed, and the NXB is subtracted. The error bar for each data shows a  $1 \sigma$  statistical uncertainty. The green and blue dash lines represent the convolved  $\beta$ -model and XB component, respectively, and the red solid line shows the combined model of these components. The magenta dash line indicates the Suzaku PSF.

**Table 1.** Fitting results of the Center region

Component (Model)	Parameter	Value*
ICM ( <i>apec</i> )	$kT$ (keV)	$3.8 \pm 0.2$
	Abundance (solar)	$0.20 \pm 0.05$
	Redshift	$0.215^{+0.007}_{-0.006}$
	Luminosity <sup>†</sup>	$15.9 \pm 0.6$
CXB ( <i>powerlaw</i> )	Photon index	1.412 (fix)
	Unabsorbed flux <sup>‡</sup>	$1.94 \times 10^{-11}$ (fix)
MWH ( <i>apec</i> )	$kT$ (keV)	$0.29^{+0.07}_{-0.05}$
	Abundance (solar)	1.0 (fix)
	Redshift	0.0 (fix)
	Unabsorbed flux <sup>‡</sup>	$6.8^{+3.1}_{-2.5} \times 10^{-15}$
LHB ( <i>apec</i> )	$kT$ (keV)	$0.10^{+0.03}_{-0.02}$
	Abundance (solar)	1.0 (fix)
	Redshift	0.0 (fix)
	Unabsorbed flux <sup>‡</sup>	$4.6^{+5.2}_{-2.2} \times 10^{-19}$
Absorption ( <i>wabs</i> )	$N_{\text{H}}$ ( $\times 10^{20}$ cm $^{-2}$ )	1.7 (fix)
$\chi^2/\text{d.o.f}$		740.25/737

\*: The errors represent the 90% confidence range.

†: The luminosity is represented in a unit of  $10^{43}$  erg s $^{-1}$  in the 0.1 – 2.4 keV band within  $r = 2$  Mpc, where the radial profile is taken into account.

‡: Flux (erg cm $^{-2}$  s $^{-1}$  deg $^{-2}$ ) are in the 2 – 10 keV band.

**Table 2.** Results of the simultaneous fit of the SW1 and SW2 region.

Parameter	SW1*	SW2*
$kT$ (keV)	$2.0 \pm 0.2$	$2.1^{+0.4}_{-0.6}$
Abundance (solar)	$0.41^{+0.17}_{-0.13}$	$0.26^{+0.21}_{-0.19}$
Redshift	$0.11 \pm 0.02$	$0.41^{+0.02}_{-0.15}$
Luminosity <sup>†</sup>	$1.25 \pm 0.07$	—
$\chi^2/\text{d.o.f}$		456.6/429

\*: The errors represent the 90% confidence range.

†: The luminosity is represented in a unit of  $10^{43}$  erg s $^{-1}$  in the 0.1 – 2.4 keV band within  $r = 2$  Mpc, where the radial profile is taken into account.

**Table 3.** Radial profiles of the SW1 and SW2 region fitted with a  $\beta$  model.

Parameter	Center*	SW1*
Core radius $r_c$ (kpc)	$450 \pm 40$	$220_{-70}^{+90}$
$\beta$ -index	$0.52 \pm 0.04$	$0.9_{-0.2}^{+0.4}$
$\chi^2/\text{d.o.f}$	46.3/22	95.5/14

\*: The errors represent the 90% confidence range.